H_2 Formation Holds the Key to Opening the Fe Coordination Sites of Nitrogenase FeMo-cofactor for Dinitrogen Activation

Yong Li,[a,b] *Wan-Lu Li,*[a] *Jin-Cheng Liu,*[a] *Jun-Bo Lu,*[c]

W. H. Eugen Schwarz,[a,d] *Lyudmila V. Moskaleva,*[b] *and Jun Li* [a,c*]

[a] *Department of Chemistry, Tsinghua University, Beijing 100084, China*
[b] *Institute of Applied and Physical Chemistry and Center for Environmental Research and Sustainable Technology, University of Bremen, Bremen 28359, Germany*
[c] *Department of Chemistry, Southern University of Science and Technology, Shenzhen 518055, China*
[d] *Department of Chemistry, University of Siegen, Siegen 57068, Germany*

* Corresponding author, E-mail: junli@tsinghua.edu.cn

Contents

Abstract

The present quantum-mechanical and molecular-mechanics study reveals the crucial roles of H_2 formation, of H_2S shift and of N_2 bond expansion in the nitrogenase process of the reduction of N_2 to NH_3. Proton and electron transfers to the Fe(C@Fe_6S_9)Mo unit of the FeMo-co complex weaken the Fe-S and Fe-H bonds and expose the **Fe** coordination sites, coupled with energy release due to H_2 generation. Thereby the two sites **Fe2** and **Fe6** become prepared for stronger N_2 adsorption, expanding and attenuating the |N≡N| bond. After subsequent detachment of H_2S from its Fe binding site into a holding site of the rearranged protein residue, the **Fe6** site becomes completely unfolded, and the N_2 triple bond becomes completely activated to an -N=N- double bond for easy subsequent hydrogenation to NH_3. We explain in particular, why the obligatory H_2 formation is an essential step in N_2 adsorption and activation.

1. Introduction

The enzyme nitrogenase can activate the strong |N≡N| bond of dinitrogen at ambient conditions, thereby providing the biological fixation of more than half of the nitrogen demanded to sustain the human population on Earth.[1, 2, 3] The total dinitrogen hydrogenation process, $N_2 + 3\,H_2 \rightarrow 2NH_3$, is slightly exothermic, and more so if activated hydrogen in the form of solvated ($H^+ + e^-$) is utilized. However, the first bond cleavage in the dinitrogen molecule (i.e. breaking |N≡N| to $\underline{N}=\underline{N}^{\bullet}$) requires a Gibbs free enthalpy of $\Delta G \approx 4.7$ eV at STP, which is almost one-half the value for full N_2 dissociation (9.7 eV).[4] Besides, the large HOMO-LUMO gap (ca. 10 eV) and the low proton affinity (5.1 eV) of N_2 make the processes of electron and proton transfer to N_2 very difficult at the beginning of the nitrogen fixation reaction. Therefore, there is great interest in the elaborate molecular-level understanding of how the nitrogenase enzyme achieves this challenging task. Elucidating the biological mechanism of nitrogen fixation would also be useful in the development of more efficient catalysts for the technical ammonia synthesis.

The stoichiometry of the nitrogenase-catalyzed nitrogen fixation reaction under ambient conditions is experimentally identified by the reaction in Eq. (1),[5]

$$N_2 + 8H^+ + 8e^- + 16ATP \rightarrow 2NH_3 + H_2 + 16ADP + 16P_i\,, \qquad (1)$$

where ATP, ADP, and P_i stand for the metabolites adenosine triphosphate, adenosine diphosphate, and an inorganic orthophosphate, respectively.

The whole nitrogenase complex consists of two proteins: (a) the homo-dimeric ‘Fe protein’ with an $[Fe_4S_4]$ subunit, responsible for the supply of electrons, and (b) the hetero-tetrameric ‘MoFe protein’ containing an $[Fe_8S_7]$ subunit (the P-cluster) and the FeMo cofactor (FeMo-co). The FeMo-co is a functional unit with a polycentric Fe_7MoCS_9 cluster (see the >[Mo(S_3 Fe_3 (C,S_3) Fe_3 S_3)Fe]– unit in the Figures below) that utilizes supplied electrons and protons (from $(H_2O)_nH^+$ chains) to reduce adsorbed N_2 and produce two NH_3 and one H_2. The rate-limiting step of the nitrogenase-catalyzed nitrogen fixation reaction (Eq. 1) is the association-dissociation of the Fe and MoFe proteins, which is proposed on the basis of kinetic studies of the biological reactions.[6, 7, 8, 9] Utilizing the energy released from the hydrolysis of coenzyme ATP, the $[Fe_4S_4]$ cluster of the Fe protein transfers electrons to the $[Fe_8S_7]$ P-cluster and passes them to the MoFe protein, where NH_3 and obligatory H_2 are created on the FeMo-co subunit.[1]

The FeMo-co as the active center of the nitrogenase MoFe protein with an interstitial central, negatively charged C atom (see the Figures below, and Fig. S1 in the Supporting Information, SI),[5, 10, 11, 12] has been isolated in three different forms: as resting/native/neutral FeMo-co^{N}, as one-electron reduced FeMo-co^{Red}, as one-electron oxidized FeMo-co^{Ox}.[13] X-ray absorption spectroscopic (XAS) observations and electron-nuclear double resonance (ENDOR) studies had first suggested that the Mo atom is in oxidation state IV and diamagnetic in all three forms, i.e. with $^{1}(4d^{2})$ electronic configuration,[14, 15, 16] while more recent HERFD-XAS, Mössbauer-Isomer-Shift and quantum-chemical computational studies identified it as Mo^{III}-$(4d^{3})$.[3, 17, 18] Based on the EPR and ENDOR results[19, 20, 21, 22, 23] and the proposed net charges, oxidation states and protonation states of the FeMo-co unit,[24, 25] one may conclude that the FeMo-co^{Ox} and FeMo-co^{N} clusters may be written with $Fe^{II}_{2}Fe^{III}_{5}Mo^{III}$ and $Fe^{II}_{3}Fe^{III}_{4}Mo^{III}$, respectively; for details see the 'Computational Model' section 1.1 in the SI.

Despite numerous experimental efforts exploring nitrogenase and its catalytic processes, many mechanistic aspects of the nitrogenase-catalyzed N_2 fixation remain unknown.[1, 2] Heretofore, there is no literature about the crystallographic structure of any intermediate such as the species with bound -N_2- or hydrogenated -N_2H_x-, due to their labile nature. Therefore theoretical investigations exploring and identifying those possible activated species and intermediates in the nitrogenase cycle have become essential.[2]

The protonation of FeMo-co has been reported in the theoretical literature based on various simplified chemical structure models. The first four possible protonation structures of FeMo-co from $\mathbf{E_0}$ to $\mathbf{E_4}$ have been deduced.[26] On experimental grounds, the key structure $\mathbf{E_4}$ has been called the "Janus intermediate", because the FeMo-co in $\mathbf{E_4}$ contains two [Fe-H-Fe] bridging hydrides, and can react in both directions releasing H_2 or N_2. Yet it was not possible to deduce an unambiguous picture of the spatial relationships of the two hydride bridges.[1, 12, 27, 28] One important point of study has been the discussion of the reductive elimination of an H_2 molecule, endothermically coupled with the cleavage of one bond of N≡N.[2,29] This point, in particular the structure of the complex with the activated N_2, the reason of the obligatory H_2 generation, and the resulting stoichiometry in reaction Eq. (1), will be theoretically studied below. We applied a hybrid quantum-chemical and molecular mechanical (QM/MM) method (sect. S1). We focused on the formation of hydrogen and ammonia molecules along reaction paths in the framework of the Lowe-Thorneley (LT) kinetic model.[5]

2. Prerequisite H^+/e^- transfers for N_2 activation and H_2 formation

Following the LT model, the protonation processes of H^+/e^- pair-transfers to FeMo-co determine the structures of the first five states, **E_0**, **E_1**, **E_2**, **E_3** and **E_4**. The first 4 steps **$E_0 \rightarrow E_1 \rightarrow E_2 \rightarrow E_3 \rightarrow E_4$** have been suggested to be the preparation phase for N_2 binding in the LT model. Some structural details of FeMo-co at **E_0** are discussed in the 'Computational Model' section S1.1 of the SI. On the basis of the published experimental and theoretical and of our current studies, the **E_0** starting structure is proposed with a net charge of −2, with oxidized form FeMo-co^{Ox}, and with a protonated hydroxyl group (see section S2). The catalytic cyclic starting from **E_0** is then here further revealed.

According to experimental studies, the accumulation of three or four H^+/e^- pairs on the FeMo-co is prerequisite for N_2 molecule adsorption and activation.[1, 19, 30] In order to identify the energetically preferred proton-accepting sites and structures of FeMo-co at each H^+/e^- transfer step, various possible geometric configurations at the **E_1** to **E_4** stages have been quantum-chemically computed. The energetically lower ones are displayed in Figs. S3 to S6 and discussed in section S2. The most probable protonated structures from **E_0** to **E_4**, likely to support the nitrogen fixation, are collected in Fig. 1a. The energetically most preferred proton accepting sites are at the three bridging S atoms Si, Sj, Sk (see structures of **E_1**, **E_{2a}**, and **E_{3a}**) for the first three protonation steps. At the level of the applied quantum-chemical density-functional approximation (BP86), the structures **E_{2b}-H_2** and **E_{3b}-H_3** are energetically comparable, only 0.1 and 0.15 eV (1 eV ≈ 96.5 kJ mol^{-1}) higher, where some H atoms are bound to Fe.

Concerning four transferred H^+/e^- pairs, we find three structures **E_{4a}**, **E_{4b}**, **E_{4c}** at comparably low energies, but different bonding modes of the hydrogen atoms, bound either to S (as 2Fe>S-H, Fe−S-H or Fe−S<2H) or to Fe (as Fe−H or 2Fe>H), all within 0.12 eV (Fig. S6). Yet it is safe to say that one or two H atoms are bound to Fe, and the other ones to S. It had been reported that in some organometallic catalysts the [Fe-H-Fe] metal-hydride bonds play a key role in the activation of the N_2 molecule.[4] Such bonds were also verified in the FeMo-co reaction cycle by ^{1,2}H and ^{95}Mo ENDOR measurements.[1, 27, 31] One can expect that iron hydride formation plays a role in the N_2 adsorption and activation by nitrogenase. However, it is an open question, whether the metal-hydride formation sets in at the second, third or fourth step of H^+/e^- addition.

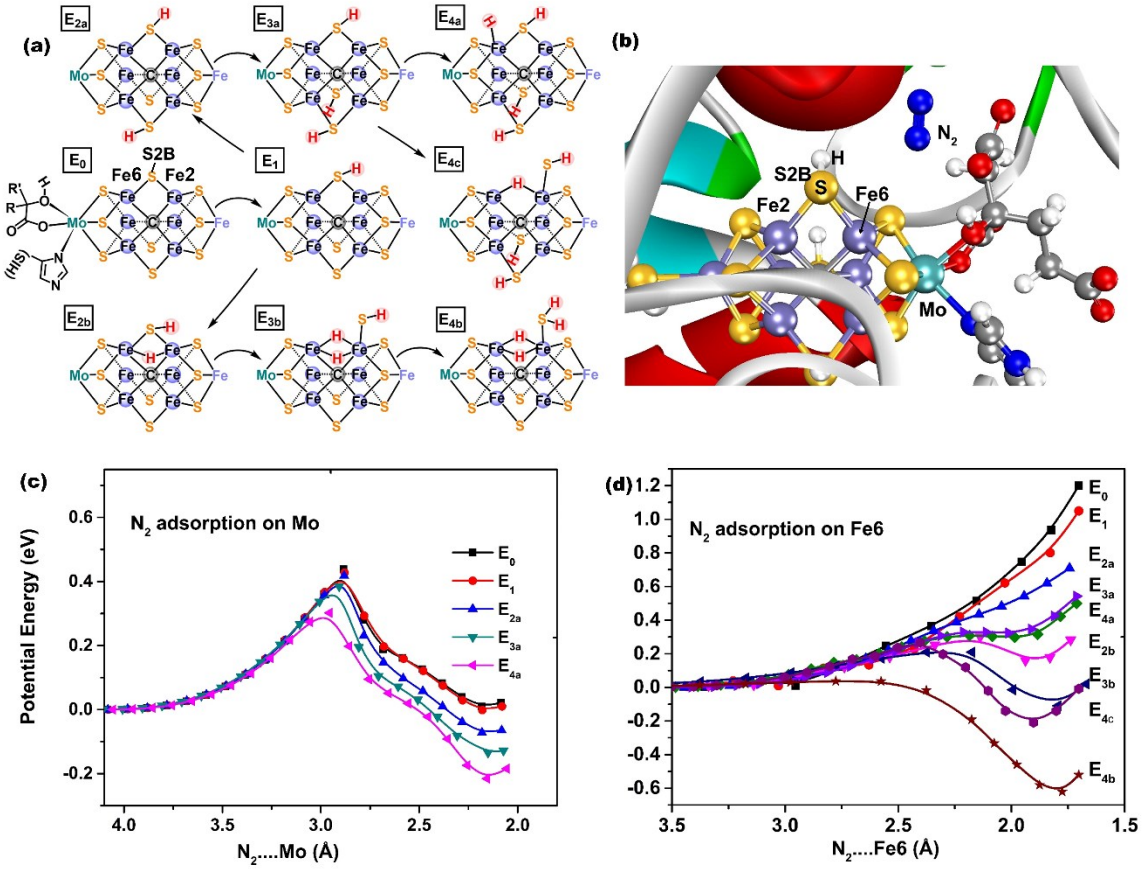

Fig. 1. (**a**) Top-left: Initiation of the nitrogen adsorption on FeMo-co with active center **Fe2-S2B-Fe6,** showing the branching path of addition of four H^+/e^- pairs to FeMo-co from state $\mathbf{E_0}$ to states $\mathbf{E_{4(a,b,c)}}$. (**b**) Top-right: The FeMo-co and the protein pocket, where the S2B bridges the Fe2 and Fe6. **(c, d)** Bottom: Energies (in eV) of adsorption of N_2 either at **Mo** (**c**, left) or **Fe6** (**d**, right) at various steps of of FeMo-co protonation, $\mathbf{E_0}$ to $\mathbf{E_4}$. "**N_2….Mo/Fe6**" is the distances (in Å) between the **Mo** or **Fe6** sites and the interacting N of the adsorbed N_2 molecule.

The central plane of the FeMo-co complex carries four, effectively negative-charged atoms, the central $C^{-0.8}$ atom surrounded by three Fe, Fe bridging $S^{-0.3}$ atoms. The first protonations occur at these sulfide atoms, weakening the Fe-S bonds. The Fe-S cleavage energy at the $\mathbf{E_0}$ stage is >2½ eV, which is reduced to >1⅓ eV afor the $\mathbf{E_1}$-$\mathbf{H_1}$ species (Fig. S7). Also the formation of Fe,Fe hydride bridge bonding (Fe-H-Fe) such as at stage $\mathbf{E_{2b}}$ weakens the Fe←$(SH)^-$ bond (dissociation energy reduced to ¼ eV, with ⅓ eV barrier). In particular, the formation of the $\mathbf{E_{3b}}$ stage completely unfolds the **Fe6** atom in S−**Fe6**<2H coordination, leading to complete exposure toward N_2 molecule adsorption. The 4th H^+/e^- transfer to FeMo-co from states $\mathbf{E_3}$ to $\mathbf{E_4}$ (i.e. $\mathbf{E_{3a}}$

to **E_{4a}**, **E_{3a}** to **E_{4c}**, or **E_{3b}** to **E_{4b}**) requires ⅔ eV (Fig. S15), which is significantly reduced upon N_2 adsorption, see below. For details see S3.

Already early experiments[4] had suggested that electrons are transferred from the Fe-cluster to the P-cluster and further to the FeMo-co, and simultaneously proton transfers to FeMo-co are achieved through water chain structures.[32] Our calculations too confirm that simultaneous 'proton-coupled electron transfer' is energetically favored over sequential electron and proton transfers (section S3 and Fig. S8). The energy gaps between the Fe or Mo d-type HOMOs of the **E_0** state of FeMo-co and the N_2-LUMOs are >2.0(?) eV before N_2 adsorption, but decrease to <1.2 eV after three to H^+/e^- transfers, facilitating the metal-d to ligand- π* 'back-donating bond stabilization' (Fig. S12).

3. N_2 activation and H_2 release

The coordinative site of **Fe6** (Figs. 1a,b and S5b) can be completely exposed after the third proton transfer to FeMo-co and forming the **E_{3b}** species with [FeH_2Fe] species. Such an exposed coordinative Fe site is favorable site for adsorption of an N_2 molecule. Potential energy curves of the N_2 molecule approaching to Mo and **Fe6** sites (adjacent to **S2B**, see Fig. 1b) in all related protonated structures of FeMo-co at each stage (**E_0** to **E_4**, Fig. 1a) were computed and are shown in Fig. 1c,d. We may conclude that the N_2 molecule is able to bind on the **Mo** or **Fe6** sites in FeMo-co at the **E_3** stage due to energy release starting at the **E_3** stage, though over an activation barrier. Apparently, the N_2 molecule shows adsorption on Fe only when a Fe hydride was formed and the Fe was exposed for coordination at the **E_3** stage. The seemingly possible N_2 binding (at **E_0** to **E_4**) on the Mo site has barriers of 0.45 eV to 0.31 eV, and adsorption energy releases of 0.0 to -0.21 eV, accompanied by cleavage of the coordinative bond between Mo and the hydroxyl group.

However, an energetically more favorable adsorption of an N_2 molecule occurs on the hydrogenated **Fe6** site of **E_3** (0.19 eV barrier, -0.22 eV adsorption energy) and **E_4** (0.0 eV barrier, -0.62 eV adsorption energy). The three isomers of **E_4** with N_2 adsorption are all formed with small or no activation barrier (< 0.31 eV, for **Mo-E_{4a}-N_2**). The energetically favorable adsorption structures at the **E_4** stage, **Mo-E_{4a}-N_2**, **Fe-E_{4b}-N_2**, **Fe-E_{4c}-N_2**, are shown in Figs. S9, S10, S11, respectively, all show slightly lengthened and weakened |N≡N| bonding; the N-N distance of

1.09 Å in the gas phase increases to 1.13 Å, which is a significant expansion for the strong triple bond.

It is experimentally known that the concomitant H_2 formation upon N_2 fixation in the nitrogenase catalytic cycle is an inevitable process. The H_2 formation from the **Mo-E_{4a}-N_2** and **Fe-E_{4c}-N_2** intermediates, however, convert them back to **Mo-E_{2a}-N_2** and **Fe-E_{2a}-N_2** structures, leading to N_2 desorption (details in section S5). In contrast, the **Fe-E_{4b}-N_2** structure exothermically forms and releases H_2, whereby the |N≡N| bond is further weakened and lengthened (from 1.13 to 1.16 Å, Fig. 2) due to the change of the N_2 adsorption mode from μ_1-η^1 to μ_2-η^1 (Figs. 2 and S11). Further release of H_2S completely exposes the coordination site of **Fe2**, strengthening the N_2 adsorption by changing the bonding mode from μ_2-η^1 to μ_2-η^2, corresponding to further weakened formal >N=N< bonding, reflected by the further N-N distance increase from 1.16 to 1.18 Å (Fig. 2). The H_2S formation is also revealed in a recent theoretical paper.[33] Energetically the H_2 formation from **E_{4b}-N_2** releases energy (ΔG = -0.21 eV) upon overcoming a barrier of 0.51 eV to **E_{4b-1}-N_2**; subsequent H_2S desorption is weakly endothermic (ΔG = +0.11 eV), binding the H_2S to the protein holding site. This allows for rearrangement of the N_2 adsorption mode from μ_2-η^1 to μ_2-η^2 mode, with an energy release of −0.24 eV. Thus the whole process is endothermic and promotes the transformation of the N≡N triple bond to the N=N double bond (Fig. 2). It reveals the relevance of the H_2 formation and release, and the intermediate H_2S formation, which together trigger the N_2 activation.

The FeMo-co is surrounded by hydrophobic groups, but a limited number of water chains are connected through the homocitrate ligand, as shown in Fig. S7. Therefore, it appears evident that the H_2S molecule hydrolyzes, forming HS^- and H_3O^+. The HS^- ion can bind in a holding site of the rearranged protein residue Q176, as revealed by a recent experimental study.[34] The coordination bonding energy of HS^- to **Fe2** is −0.51 eV, more than the binding energy of H_2S to **Fe2** (−0.11 eV, the respective desorption was mentioned above). It implies that the release of the HS^- anion would not occur without the binding in the protein pocket.

The accumulation of H^+/e^- pairs on FeMo-co increases its reduction potential and hence the ability to bind the N_2 molecule, as shown in Fig. 1c,d and further discussed in section S4. Concomitantly the translocation of H^+/e^- pairs also supports the breaking of the Fe-S coordinative bond, thereby exposing the coordinative Fe site for N_2 adsorption. The proposed detailed activation mechanism was depicted in Fig. 2. We summarize: the H^+/e^- transfer

promotes the weakening and cleavage of the Fe-S bond at the **E_1** and **E_2** stages and further facilitates the exposure of the Fe atom and the formation of Fe hydride bonding. After 3 H^+/e^- couple pairs were successfully transferred to FeMo-co (**E_{3b}**), the **Fe6** coordinative site is completely exposed, promoting the adsorption of the N_2 molecule as straightened out in Fig. 2. The formation of H_2S at the **E_4** stage induces the cleavage of the Fe2-S bond, completely exposing the **Fe2** coordinative site for further activating the adsorbed N_2. The exposure of the Fe coordinative site plays the key role in the nitrogen adsorption and activation.

To further support these points, we performed chemical bonding analyses along the activation path from **E_{3b}-N_2** to **E_4-N_2**, illustrating the change of the electronic structure during the activation process. Wiberg bond order (BO) indices and Weinhold effective atomic charges from so-called natural population analysis (NPA) are listed in Table S3. The formal triple bond of the free isolated |N≡N| molecule has BO = 3.00; this is effectively converted into a double bond (BO = 2.24, see also Fig. 2) via electron donation from the adjacent **Fe6** and **Fe2** atoms. Namely, despite of the low electronegativity of iron (EN = 1.6, while S and C have EN = 2.4 to 2.5), the Fe atoms are negatively charged in FeMo-co, because of the formal C^{-4} unit at the center, which indicates the importance of the unusual anionic carbon in the middle of a slightly deformed Fe_6 octahedron. The N=N π type bonding orbitals and its π^* antibonding counterparts are shown for the various intermediates in Fig. S16. From **E_{3b}-N_2** to **$E_{4b\text{-}1}$-N_2**, the π^* antibonding orbital contours are basically unchanged, but due to the 'back-donation' of electrons from the d-shells of the Fe6 atom, the total π^* occupation increases from 0 for the free N_2 to ca. ½e. This weakens, expands and activates the |N≡N| triple bond the electronic charge density rearrangement to –N=N| . It is consistent with the charge analysis of **Table S3**. The existence of the central formal carbon anion as an electronic charge supplier via Fe to N_2 in addition to the formal Fe cations acting as acceptors for the N2 lone-pairs appears instrumental. At the E4-N_2 stage, upon release of the two Fe bridge-H atoms as H_2, the two Fe bind the N1 atom through their Fe-3d orbitals.

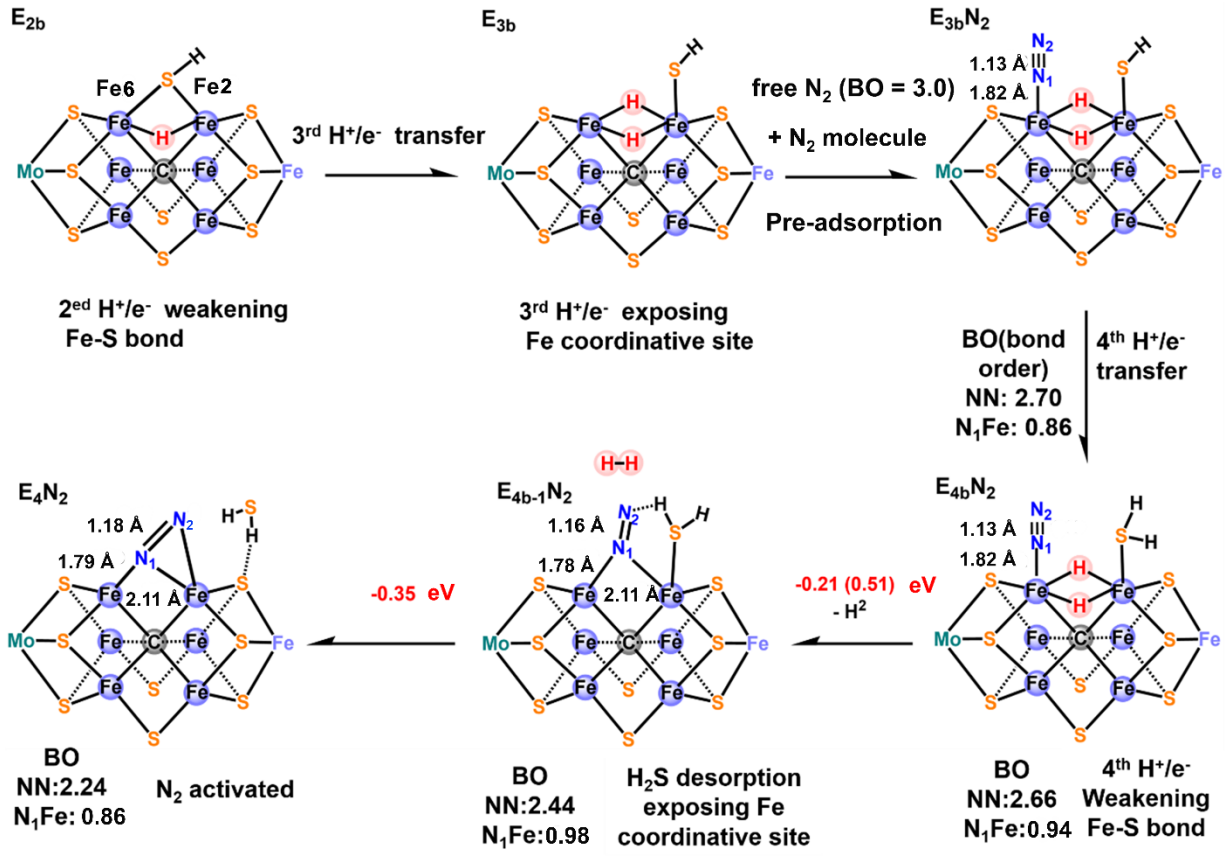

Fig. 2. Suggested reaction mechanism of the N_2 adsorption and activation. The pink spheres labeled with red H are the hydrogen atoms that form H_2 molecule. (BO = bond order. Energies in eV. Bond lengths in Å. Free N_2 has BO = 3.00 and bond length = 1.09Å.)

The lowest energy paths at the beginning are the **'a-Fe'** and **'a-Mo'** ones through structures **E_0→E_1→E_{2a}→E_{3a}** , while the **'b-Fe'** path **E_0→E_1→E_{2b}→E_{3b}** (discussed in sections S4 and S5 and Fig. S15) is higher by 0.10 eV and 0.16 eV at the **E_2** and **E_3** states, respectively. However, the N_2 adsorption on **E_{3b}** forming **E_{3b}-N_2**, dramatically lowers the energy by 0.49 eV, making the **b-Fe** path more favorable than **a-Fe** and **a-Mo** paths, as shown by Fig. 1d. Fig. S15 shows that the **b-Fe** path has the overall lower activation barriers.

4. Hydrogenation of the activated N_2

The hydrogenation of the activated dinitrogen starts at the **E_4-N_2** structure. N-N bond-breaking of the adsorbed activated N_2 molecule upon direct hydrogenation of the terminal N atom turns out

as energetically unfavorable. A potential energy surface scan of the cleavage of the N=N double bond of the activated N_2 on FeMo-co showed a high barrier of ~1.72 eV. However, splitting off an HS^- group and storing it in the holding site of the protein residue Q176 is favorable. For reasons of computational expenses, we kept the H_2S together with a H_2O molecule just in the surrounding of the reaction center. All barriers of H^+/e^- transfer were estimated for reactions of type

$$H_3O^+ + (NN)\cdot H_x[FeMo\text{-}co]^- \rightarrow H_2O + (NN)\cdot H_{x+1}[FeMo\text{-}co],$$

where x = 0 – 5. The potential energy curves of proton transfer from H_3O^+ to the acceptor sites are listed in Fig. S17. No barrier has been found for any protonation reaction on the **b-Fe** path. Any barrier must be due to electron transfer from the electron source to the neutral $(NN)\cdot H_{x+1}$[FeMo-co] species, which is not easy to determine computationally.

We have computed the energy profiles of the subsequent intermediates to determine the sequence of N_2 hydrogenation and NH_3 formation in this biocatalytic process. The energetically most favored reaction path after the initial **b-Fe** steps is sketched in Figs. 3 (mechanism) and 4 (energies) (more details in section S5, and Fig. S15). The H^+/e^- pair transfer to FeMo-co at $\mathbf{E_5}$ hydrogenates the activated -N=N- species at the terminal N atom, forming an -N=N-H intermediate (Fig. 3) which however requires an activation by +0.48 eV Gibbs free enthalpy ΔG. The next hydrogenation step at $\mathbf{E_6}$ leads to $-NNH_2$, requiring only ΔG = + 0.18 eV. The first NH_3 molecule is then generated after a H^+/e^- pair transfer at $\mathbf{E_7}$, releasing ΔG = −0.35 eV. (Alternative paths of $-NH-NH_2$ formation instead of $-N-NH_3$ were evaluated as well, and turned out as unfavorable with a higher energy of +0.56 eV.) Namely, after the previous hydrogenation steps, one N atom bridges two Fe centers, the other N interacts with a coordinated H_2S through a hydrogen bond. A hydrogen atom transfers from H_2S to the bridging N atom about a low barrier of +0.16 eV, releasing an energy of −0.07 eV ($\mathbf{E_{7a}}\rightarrow\mathbf{E_7}$ in Fig. 4 and Fig. S11). The last H^+/e^- pair is transferred at $\mathbf{E_8}$ to the bridging N forming an $-NH_2$ intermediate species under release of −0.81 eV. Then the above mentioned HS^- species coordinates back to the **Fe2** atom. In next reaction step, the H atom from the SH^- ligand transfers to $-NH_2$ generating the second NH_3 molecule over a low barrier of +0.04 eV, releasing −0.98 eV of energy.

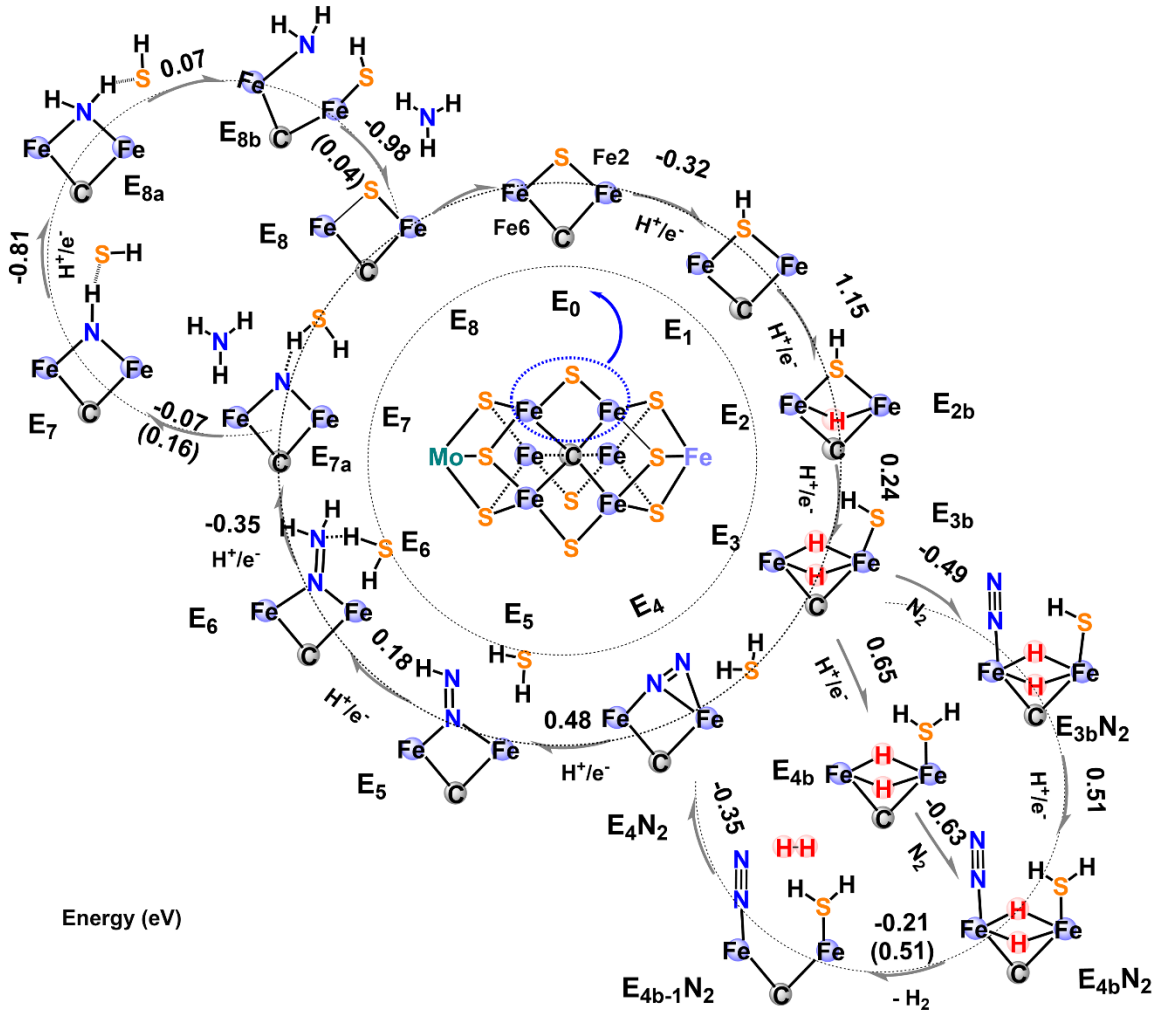

Fig. **3**. Proposed nitrogen fixation mechanism along the **b-Fe** path of the nitrogenase catalytic cycle, showing in total eight H^+/e^- pair transfers, one N_2 adsorption, one H_2 formation, the N_2 activation and hydrogenation, and the formation of two NH_3. (Gibbs free reaction enthalpies in eV. Numbers in parentheses represent the reaction activation barriers in eV.)

At this point, the catalytic cycle is completed. The FeMo-co is regenerated, H_2 and NH_3 are released with a 1:2 product ratio. After a first direct hydrogenation, the next fife H atoms are transferred from SH_2 and SH^- ligands to -NNH, yielding at first -NH··SH and NH_3, and then the second NH_3. Our theoretically derived mechanism of nitrogen adsorption and hydrogenation is consistent with the experimentally derived LT model, consisting of 8 H^+/e^- pair transfer steps

from $\mathbf{E_0}$ to $\mathbf{E_8}$. For comparison, two alternative starting pathways of N_2 activation, the **a-Fe** and the **a-Mo** paths, have higher activation barriers.

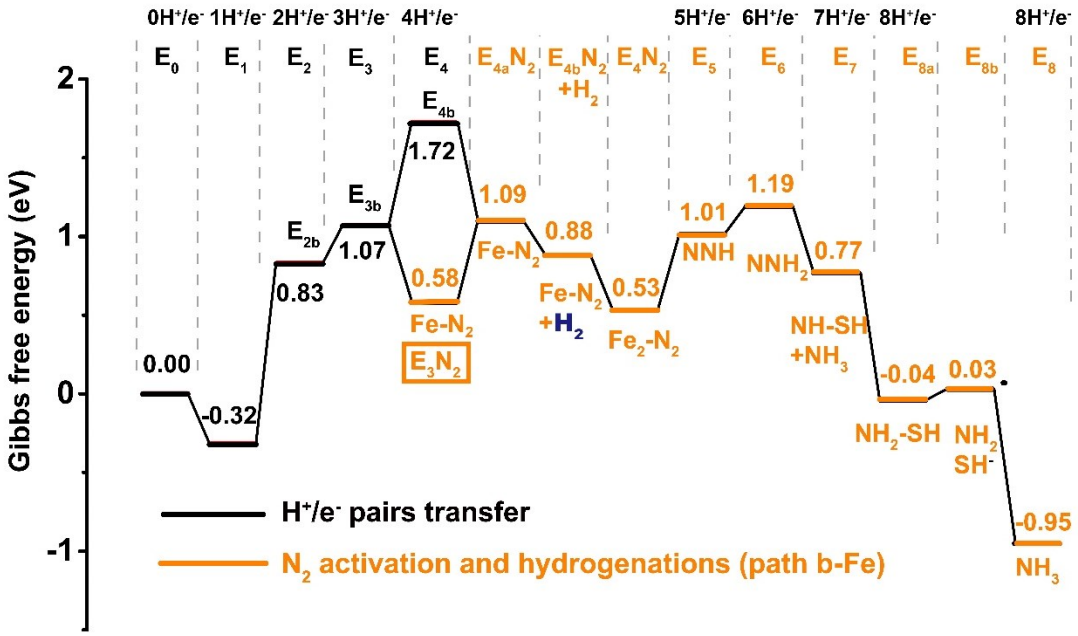

Fig. 4. Computed (DFT-BP86) Gibbs free energy profile (in eV) of nitrogen fixation at FeMo-co, including the following steps: eight H^+/e^- pair transfers, N_2 adsorption, H_2 formation, N_2 activation, hydrogenation of N_2 and formation of two NH_3, corresponding to the Lowe-Thorneley model.

5. Conclusions

We have theoretically investigated the accumulation of H^+/e^- pairs at the FeMo-co sites, the N_2 adsorption, the H_2 formation, the N_2 activation, and the hydrogenation of the activated N_2. Coupled with electron transfers, the first proton prefers binding at the bridge-S2B site, the second and third protons bind between **Fe2** and **Fe6** forming an $>Fe_2H_2$ hydride species, and breaking the Fe-SH coordinative bond, which leads to complete exposure of the **Fe6** coordinative site for the subsequent N_2 adsorption. After favorable N_2 adsorption on the **Fe6** site of the $>Fe_2H_2$ hydride, the fourth proton prefers binding at the S2B site as well, forming an H_2S molecule that will hydrolyze into HS^- and H^+. Such a chemical process leads to the exposure of

the **Fe2** coordinative site. The H_2 formation weakens the N≡N bond (the bond length increases from 1.13 to 1.16 Å, see **Fig. 2**) by a change of the N_2 adsorption mode from μ_1-η^1 to μ_2-η^1. Further release of H_2S completely exposes the coordination site of **Fe2,** leading to the N2 adsorption change from the μ_2-η^1 to the μ_2-η^2 structure and results in the increased bond length of the N_2 from 1.16 to 1.18 Å. We confirm that the obigatory generation of H_2 promotes the activation of the N_2 by exposing the Fe coordinantion sites. Our studies also show that the polarization of water molecules can promote the adsorption and activation of nitrogen. The N_2 activation and its subsequent hydrogenation processes proposed here can be summarized as:

E$_4$(–N≡N) → **E**$_4$(>N=N) +H_2↑→ **E**$_4$(–N=N– + H_2S) + H → **E**$_5$(–N=NH + H_2S) + H → **E**$_6$(=N-NH_2 + H_2S) + H → **E**$_7$(=N··HSH + NH_3 ↑) → **E**$_{7'}$(=HN··HS)+ H → **E**$_8$(NH_3↑)

Our theoretical study hence reveals the nature of the nitrogen fixation mechanism catalyzed by nitrogenase.

Acknowledgments

This work was supported by the National Natural Science Foundation of China (NSFC grants 22033005, 21590792, and 91645203) and the Guangdong Key Laboratory of Catalytic Chemistry. We thank the Supercomputer centers at Tsinghua National Laboratory for Information Science and Technology and North-German Supercomputing Alliance (HLRN) for providing computational resources.

Author contributions

J. L. designed the project. Y. L. performed the computational work; W-L. L. performed the NBO analysis. Y. L., W-L. L., J-C. L., J-B. L., provided insightful discussion to design the theoretical model. Y. L., W. H. E. S., L. V. M., and J. L co-wrote the manuscript.

Competing interests

The authors declare no conflicts of interest

References

1. Hoffman BM, Lukoyanov D, Yang Z-Y, Dean DR, Seefeldt LC. Mechanism of Nitrogen Fixation by Nitrogenase: The Next Stage. *Chem Rev* 2014, **114**(8)**:** 4041-4062.
2. Dance I. Computational Investigations of the Chemical Mechanism of the Enzyme Nitrogenase. *ChemBioChem* 2020, **21**(12)**:** 1671-1709.
3. Van Stappen C, Decamps L, Cutsail GE, Bjornsson R, Henthorn JT, Birrell JA*, et al.* The Spectroscopy of Nitrogenases. *Chem Rev* 2020, **120**(12)**:** 5005-5081.
4. Jia H-P, Quadrelli EA. Mechanistic aspects of dinitrogen cleavage and hydrogenation to produce ammonia in catalysis and organometallic chemistry: relevance of metal hydride bonds and dihydrogen. *Chem Soc Rev* 2014, **43**(2)**:** 547-564.
5. Simpson F, Burris R. A nitrogen pressure of 50 atmospheres does not prevent evolution of hydrogen by nitrogenase. *Science* 1984, **224**(4653)**:** 1095-1097.
6. Lowe DJ, Thorneley RN. The mechanism of Klebsiella pneumoniae nitrogenase action. Pre-steady-state kinetics of H_2 formation. *Biochem J* 1984, **224**(3)**:** 877-886.
7. Lowe DJ, Thorneley RNF. The mechanism of Klebsiella pneumoniae nitrogenase action. The determination of rate constants required for the simulation of the kinetics of N_2 reduction and H_2 evolution. *Biochem J* 1984, **224**(3)**:** 895-901.
8. Thorneley RNF, Lowe DJ. The mechanism of Klebsiella pneumoniae nitrogenase action. Pre-steady-state kinetics of an enzyme-bound intermediate in N_2 reduction and of NH_3 formation. *Biochem J* 1984, **224**(3)**:** 887-894.
9. Thorneley RNF, Lowe DJ. The mechanism of Klebsiella pneumoniae nitrogenase action. Simulation of the dependences of H_2-evolution rate on component-protein concentration and ratio and sodium dithionite concentration. *Biochem J* 1984, **224**(3)**:** 903-909.
10. Spatzal T, Aksoyoglu M, Zhang L, Andrade SLA, Schleicher E, Weber S*, et al.* Evidence for Interstitial Carbon in Nitrogenase FeMo Cofactor. *Science* 2011, **334**(6058)**:** 940-940.
11. Lancaster KM, Hu Y, Bergmann U, Ribbe MW, DeBeer S. X-ray Spectroscopic Observation of an Interstitial Carbide in NifEN-Bound FeMoco Precursor. *J Am Chem Soc* 2013, **135**(2)**:** 610-612.
12. Seefeldt LC, Yang Z-Y, Lukoyanov DA, Harris DF, Dean DR, Raugei S*, et al.* Reduction of Substrates by Nitrogenases. *Chem Rev* 2020.
13. Igarashi RY, Seefeldt LC. Nitrogen Fixation: The Mechanism of the Mo-Dependent Nitrogenase. *Crit Rev Biochem Mol Biol* 2003, **38**(4)**:** 351-384.
14. Corbett MC, Tezcan FA, Einsle O, Walton MY, Rees DC, Latimer MJ*, et al.* Mo K- and L-edge X-ray absorption spectroscopic study of the ADP.AlF4--stabilized nitrogenase complex: comparison with MoFe protein in solution and single crystal. *J Synchrotron Radiat* 2005, **12**(1)**:** 28-34.
15. Hedman B, Frank P, Gheller SF, Roe AL, Newton WE, Hodgson KO. New structural insights into the iron-molybdenum cofactor from Azotobacter vinelandii nitrogenase through sulfur K and molybdenum L x-ray absorption edge studies. *J Am Chem Soc* 1988, **110**(12)**:** 3798-3805.
16. Venters RA, Nelson MJ, McLean PA, True AE, Levy MA, Hoffman BM*, et al.* ENDOR of the resting state of nitrogenase molybdenum-iron proteins from Azotobacter vinelandii, Klebsiella pneumoniae, and Clostridium pasteurianum. Proton, iron-57, molybdenum-95, and sulfur-33 studies. *J Am Chem Soc* 1986, **108**(12)**:** 3487-3498.

17. Bjornsson R, Lima FA, Spatzal T, Weyhermuller T, Glatzel P, Bill E*, et al.* Identification of a spin-coupled Mo(iii) in the nitrogenase iron-molybdenum cofactor. *Chem Sci* 2014, **5**(8)**:** 3096-3103.
18. Bjornsson R, Neese F, DeBeer S. Revisiting the Mössbauer Isomer Shifts of the FeMoco Cluster of Nitrogenase and the Cofactor Charge. *Inorg Chem* 2017, **56**(3)**:** 1470-1477.
19. Burgess BK, Lowe DJ. Mechanism of Molybdenum Nitrogenase. *Chem Rev* 1996, **96**(7)**:** 2983-3012.
20. Harris TV, Szilagyi RK. Comparative Assessment of the Composition and Charge State of Nitrogenase FeMo-Cofactor. *Inorg Chem* 2011, **50**(11)**:** 4811-4824.
21. Conradson SD, Burgess BK, Holm RH. Fluorine-19 chemical shifts as probes of the structure and reactivity of the iron-molybdenum cofactor of nitrogenase. *J Biol Chem* 1988, **263**(27)**:** 13743-13749.
22. Yoo SJ, Angove HC, Papaefthymiou V, Burgess BK, Münck E. Mössbauer Study of the MoFe Protein of Nitrogenase from Azotobacter vinelandii Using Selective 57Fe Enrichment of the M-Centers. *J Am Chem Soc* 2000, **122**(20)**:** 4926-4936.
23. True AE, Nelson MJ, Venters RA, Orme-Johnson WH, Hoffman BM. Iron-57 hyperfine coupling tensors of the FeMo cluster in Azotobacter vinelandii MoFe protein: determination by polycrystalline ENDOR spectroscopy. *J Am Chem Soc* 1988, **110**(6)**:** 1935-1943.
24. Pickett CJ, Vincent KA, Ibrahim SK, Gormal CA, Smith BE, Best SP. Electron-Transfer Chemistry of the Iron–Molybdenum Cofactor of Nitrogenase: Delocalized and Localized Reduced States of FeMoco which Allow Binding of Carbon Monoxide to Iron and Molybdenum. *Chem Eur J* 2003, **9**(1)**:** 76-87.
25. Huang HQ, Kofford M, Simpson FB, Watt GD. Purification, composition, charge, and molecular weight of the FeMo cofactor from azotobacter vinelandii nitrogenase. *J Inorg Biochem* 1993, **52**(1)**:** 59-75.
26. Kästner J, Blöchl PE. Ammonia Production at the FeMo Cofactor of Nitrogenase: Results from Density Functional Theory. *J Am Chem Soc* 2007, **129**(10)**:** 2998-3006.
27. Lukoyanov D, Yang Z-Y, Dean DR, Seefeldt LC, Hoffman BM. Is Mo Involved in Hydride Binding by the Four-Electron Reduced (E4) Intermediate of the Nitrogenase MoFe Protein? *J Am Chem Soc* 2010, **132**(8)**:** 2526-2527.
28. Cao L, Ryde U. What Is the Structure of the E4 Intermediate in Nitrogenase? *J Chem Theory Comput* 2020, **16**(3)**:** 1936-1952.
29. Raugei S, Seefeldt LC, Hoffman BM. Critical computational analysis illuminates the reductive-elimination mechanism that activates nitrogenase for N2 reduction. *Proc Natl Acad Sci* 2018, **115**(45)**:** E10521-E10530.
30. Wilson PE, Nyborg AC, Watt GD. Duplication and extension of the Thorneley and Lowe kinetic model for Klebsiella pneumoniae nitrogenase catalysis using a mathematica software platform. *Biophy Chem* 2001, **91**(3)**:** 281-304.
31. Igarashi RY, Laryukhin M, Dos Santos PC, Lee H-I, Dean DR, Seefeldt LC*, et al.* Trapping H- Bound to the Nitrogenase FeMo-Cofactor Active Site during H2 Evolution: Characterization by ENDOR Spectroscopy. *J Am Chem Soc* 2005, **127**(17)**:** 6231-6241.
32. Dance I. The pathway for serial proton supply to the active site of nitrogenase: enhanced density functional modeling of the Grotthuss mechanism. *Dalton Trans* 2015, **44**(41)**:** 18167-18186.

33. Dance I. How feasible is the reversible S-dissociation mechanism for the activation of FeMo-co, the catalytic site of nitrogenase? *Dalton Trans* 2019, **48**(4)**:** 1251-1262.
34. Sippel D, Rohde M, Netzer J, Trncik C, Gies J, Grunau K*, et al.* A bound reaction intermediate sheds light on the mechanism of nitrogenase. *Science* 2018, **359**(6383)**:** 1484-1489.